

RESEARCH ARTICLE

Molecular Mechanisms of 2, 3', 4, 4', 5-Pentachlorobiphenyl-Induced Thyroid Dysfunction in FRTL-5 Cells

Hui Yang^{1☯‡}, Huanhuan Chen^{1☯‡}, Hongwei Guo¹, Wen Li¹, Jinmei Tang¹, Bojin Xu¹, Minne Sun¹, Guoxian Ding², Lin Jiang¹, Dai Cui¹, Xuqin Zheng¹, Yu Duan^{1*}

1 Department of Endocrinology, First Affiliated Hospital of Nanjing Medical University, Nanjing, China, **2** Department of Gerontology, First Affiliated Hospital of Nanjing Medical University, Nanjing, China

☯ These authors contributed equally to this work.

‡ These authors are co-first authors on this work.

* duanyu@medmail.com.cn



OPEN ACCESS

Citation: Yang H, Chen H, Guo H, Li W, Tang J, Xu B, et al. (2015) Molecular Mechanisms of 2, 3', 4, 4', 5-Pentachlorobiphenyl-Induced Thyroid Dysfunction in FRTL-5 Cells. *PLoS ONE* 10(3): e0120133. doi:10.1371/journal.pone.0120133

Academic Editor: Hiroyoshi Ariga, Hokkaido University, JAPAN

Received: August 14, 2014

Accepted: January 19, 2015

Published: March 19, 2015

Copyright: © 2015 Yang et al. This is an open access article distributed under the terms of the [Creative Commons Attribution License](https://creativecommons.org/licenses/by/4.0/), which permits unrestricted use, distribution, and reproduction in any medium, provided the original author and source are credited.

Data Availability Statement: All files are available from the Dryad database (doi:10.5061).

Funding: This work was supported by the Natural Science Foundation of China (NSFC 81170726), Key Medical Talents from Jiangsu Provincial Health Bureau of China (Duanyu 2011), and the Program for Development of Innovative Research Team in the First Affiliated Hospital of NJMU (20110312). The project was funded by the Priority Academic Program Development of Jiangsu Higher Education Institutions. The funders had no role in study design, data collection and analysis, decision to publish, or preparation of the manuscript.

Abstract

Polychlorinated biphenyls (PCBs) can severely interfere with multiple animals and human systems. To explore the molecular mechanisms underlying 2, 3', 4, 4', 5-pentachlorobiphenyl (PCB118)-induced thyroid dysfunction, Fischer rat thyroid cell line-5 (FRTL-5) cells were treated with either different concentrations of PCB118 or dimethyl sulfoxide (DMSO). The effects of PCB118 on FRTL-5 cells viability and apoptosis were assessed by using a Cell Counting Kit-8 assay and apoptosis assays, respectively. Quantitative real-time polymerase chain reaction was used to quantify protein kinase B (Akt), Forkhead box protein O3a (FoxO3a), and sodium/iodide symporter (NIS) mRNA expression levels. Western blotting was used to detect Akt, phospho-Akt (p-Akt), FoxO3a, phospho-FoxO3a (p-FoxO3a), and NIS protein levels. Luciferase reporter gene technology was used to detect the transcriptional activities of FoxO3a and NIS promoters. The effects of the constitutively active Akt (CA-Akt) and dominant-negative Akt (DN-Akt) plasmids on p-Akt, p-FoxO3a, and NIS levels were examined in PCB118-treated FRTL-5 cells. The effects of FoxO3a siRNA on FoxO3a, p-FoxO3a, and NIS protein levels were examined in the PCB118-treated FRTL-5 cells. The effects of pcDNA3 (plasmid vectors designed for high-level stable and transient expression in mammalian host)-FoxO3a on NIS promoter activity were examined in the PCB118-treated FRTL-5 cells. Our results indicated that relatively higher PCB118 concentrations can inhibit cell viability in a concentration- and time-dependent manner. Akt, p-Akt, and p-FoxO3a protein or mRNA levels increased significantly in PCB118-treated groups and NIS protein and mRNA levels decreased considerably compared with the control groups. FoxO3a promoter activity increased significantly, whereas NIS promoter activity decreased. These effects on p-FoxO3a and NIS could be decreased by the DN-Akt plasmid, enhanced by the CA-Akt plasmid, and blocked by FoxO3a siRNA. The overexpressed FoxO3a could reduce NIS promoter activity. Our results suggested that PCB118 induces thyroid cell dysfunction through the Akt/FoxO3a/NIS signaling pathway.

Competing Interests: The authors have declared that no competing interests exist.

Introduction

Polychlorinated biphenyls (PCBs) are a type of typical environmental endocrine disruptors present in persistent organic pollutants. Because of their stable chemical properties and perfect insulativity, they were widely used in many industries as flame retardants, transformers, capacitors, lubricants, and plasticizers until their production was banned in 1979. However, owing to their lipophilic and biological persistence, significant concentrations of PCBs still exist in the environment. Because they can easily accumulate in adipose tissue, they gradually accumulate up the food chain, and affect human health by damaging multiple organs. Numerous research studies have indicated that long-term exposure to PCBs produces adverse effects on the immune, reproductive, and nervous systems. PCBs have also been associated with hepatotoxicity and lipotoxicity, especially in newborns, young children, and adolescents [1–4]. In addition, PCBs are thought to affect thyroid function. When harbor seals and Beluga whales were exposed to various organochlorine compounds, mainly PCBs, a high incidence of goiter was observed [5]. It was declared that PCBs could interfere with thyroid hormone synthesis, secretion, transportation, and metabolism. Our early findings suggested that low concentrations of 2,3',4,4',5-pentachlorobiphenyl or continuous exposure in animal models to polychlorinated biphenyl 118 (PCB118) induced abnormal thyroid morphology, dramatically decreasing the expression of thyroidal sodium/iodide symporter [NIS or solute carrier family 5, member 5 (SLC5A5)] at the transcriptional level [6]; however, the underlying mechanism was unknown [7–9].

NIS is located on the outer membrane of thyrocytes. Its function is to pump sodium out of follicular cells while pumping iodide into the cells, thus constituting the first step in the biosynthesis of iodine-containing hormones such as triiodothyronine and thyroxine [10] (Fig. 1A). NIS activity is sensitive to both iodine availability and thyroid-stimulating hormone (TSH) stimulation, and without it, iodine would not be imported into the follicular cells in sufficiently high concentrations to produce adequate amounts of thyroxine [11]. Numerous studies have indicated that cyclic adenosine monophosphate, protein kinase A, and protein kinase C are involved in mediating NIS transcription activity [10], but Kogai et al. also reported that decreased NIS mRNA expression and NIS trafficking to the plasma membrane were found in differentiated thyroid cancers, which may be attributed to the activation of the insulin/phosphoinositide-3-kinase (PI3K)/Akt signaling pathway [11]. In addition, the activated PI3K/Akt pathway

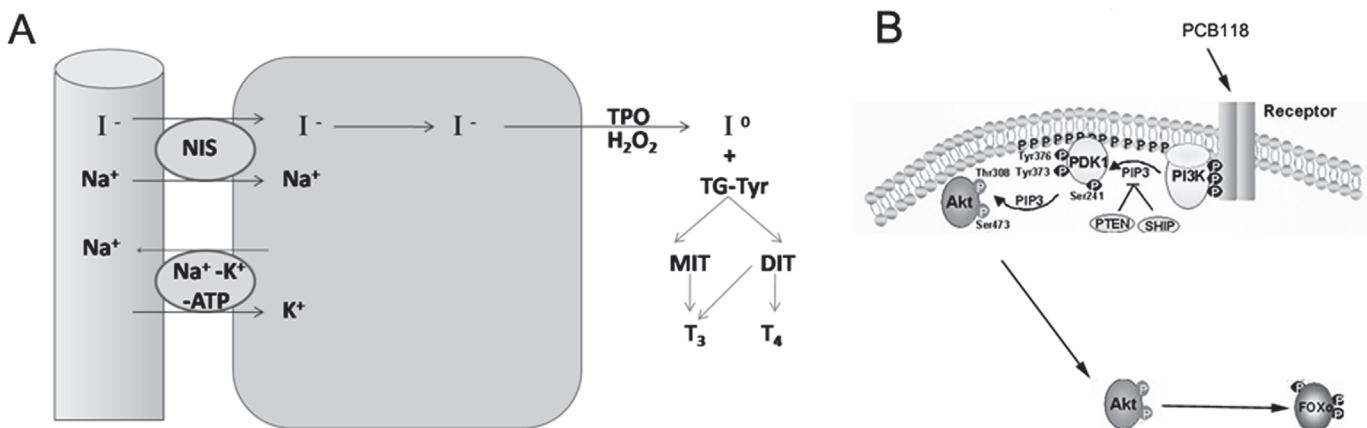


Fig 1. Functional diagrams of NIS and the PI3K/Akt/FoxO3a pathway. NIS is located on the outer membrane of the thyrocyte. Its function is to pump sodium out of the follicular cells while pumping iodide into the follicular cells (A); PCB118 stimulates cells, activates the PI3K/Akt signaling pathway, and increases Akt phosphorylation levels, after which p-Akt phosphorylates its downstream target gene FoxO3a (B).

doi:10.1371/journal.pone.0120133.g001

inhibits NIS expression and function in thyrocytes [12]. Akt (or protein kinase B), a serine/threonine kinase, is one of the primary kinases activated by PI3K and is a central regulator of cellular processes, including proliferation, differentiation, migration, survival, metabolism, and therapeutic resistance [13–17]. On the other hand, Forkhead box protein O3a (FoxO3a), which belongs to Forkhead transcription factors of the FoxO subfamily (FoxOs), is one of the most important downstream targets of the PI3K/Akt pathway [18], which is reportedly involved in cell cycle arrest [19], apoptosis [20], and the oxidative stress response [21,22]. FoxO3a localizes in the nucleus, where it activates the transcription of target genes and is phosphorylated by activated Akt; phosphorylated FoxO3a transfers to the cytoplasm where its transcriptional activity is inhibited [23] (Fig. 1B). Although it has been confirmed that several transcription factors regulate NIS expression by binding to a NIS promoter, such as β -catenin, Pax8, p53 [24,25], it has not been confirmed whether FoxO3a plays a role in NIS expression.

Fischer rat thyroid cell line-5 (FRTL-5) is a functional clone of cells that behave in a manner similar to normal thyrocytes *in vitro* and has been used as a model for studying thyroid cell functions relevant to human pathophysiology. It is the most preferred and frequently used thyroid cell line for its simplicity, accessibility, and ability of allowing permanent transfections [26]. Previous studies showed that treatment with the non-steroidal anti-inflammatory drug sulindac sulfide reverses the PI3K/Akt-mediated cytoplasmic accumulation of FoxO3a and restores its transcriptional activity in FRTL-5 cells [27]; The aforementioned results indicated that the activity of FRTL-5 cells was involved in the PI3K/Akt/FoxO3a pathway.

Here, we proposed that PCBs may induce abnormal NIS expression by activating the PI3K/Akt pathway and result in thyroid dysfunction. We selected PCB118 to investigate the molecular mechanisms underlying PCB-induced thyroid dysfunction in FRTL-5 rat cells in our study.

Materials and Methods

Materials

FRTL-5 cells were kindly provided by Dr. Zheng Xuqin (Department of Endocrinology, First Affiliated Hospital of Nanjing Medical University) [28], who was kindly gifted these cells by Professor Michael Derwahl (Department of Medicine, St. Hedwig Hospital) [29]. Coon's modified Ham's F-12 medium, transferrin, bovine insulin, hydrocortisone, somatostatin, glycyl-L-histidyl-L-lysine acetate, and bovine TSH were purchased from Sigma-Aldrich (USA). Newborn calf serum was purchased from Gibco (USA). Penicillin and streptomycin were purchased from HyClone (USA). PCB118 (purity: 100%, analyzed using GC/MS) was purchased from AccuStandard (USA) and was dissolved initially in 612 μ L dimethyl sulfoxide (DMSO) and maintained as a 25 mM stock solution in the dark. When needed, this solution was diluted to the required concentration with culture media. The final concentration of DMSO in culture medium was maintained below 0.1%.

Cell culture

FRTL-5 cells were maintained in Coon's modified Ham's F-12 medium supplemented with 5% newborn calf serum, 100-U/mL penicillin, 100- μ g/mL streptomycin and a six-hormone mixture containing 10- μ g/mL bovine insulin, 0.36-ng/mL hydrocortisone, 5- μ g/mL transferrin, 2-ng/mL glycyl-L-histidyl-L-lysine acetate, 10-ng/mL somatostatin and 1-mU/mL bovine TSH. The cells were maintained in 5% CO₂ at 37°C and passaged every 7–10 days as described previously [30]. We observed cells under a microscope, and the experiments were initiated when the proportion of adherent cells on the culture plate approached 80%. When seeding cells, we digested and counted cells to ensure that an equal number of cells were seeded into each well.

Cell viability assay

The Cell-Counting Kit-8 (CCK-8; Beyotime, China) viability assay was used as an index of cell viability according to the manufacturer's recommendations. In brief, FRTL-5 cells were seeded in 96-well plates (100 μ L, 1×10^4 cells/well) and cultured overnight. Cells were divided into the following three groups: (1) blank control (BC) group, in which cells were incubated with culture medium without DMSO or PCB118; (2) DMSO (solvent) control group, in which cells were incubated with culture medium and DMSO; and (3) PCB118 treated group, in which cells were incubated with culture medium and PCB118; the latter was further subdivided according to the final PCB118 concentrations of 0.025, 0.25, 2.5, 25, 250, 2500, and 25000 nM, respectively. Cells were separately incubated for 24, 48, or 72 h. Subsequently, 10 μ L of CCK8 was added to each well, and the cells were incubated for a further 2–3 h. Under the action of mitochondrial dehydrogenase in cells, CCK8 could be reduced to a yellow carapace product with high water solubility named as formazan, and the amount of formazan produced is positively correlated with cell viability. The absorbance was determined at 450 nm using a microplate reader, and the absorbance value indirectly reflected the number of viable cells. We then measured the absorbance values of the reaction product formazan at 450 nm for each well using a microplate reader. The relative level of cell viability in each group of cells was calculated according to a previously described formula: $P = A1/A2 \times 100\%$ in which P was relatively cell viability ratio; A1 was mean absorbance value of PCB118-treated cells; and A2 was mean absorbance value of solvent control cells [31]. All determinations were performed in quintuplicate.

Cell apoptosis assay

On the basis of the results of the cell viability assay, the PCB118-treated groups with concentrations of 0.025–25 nM were selected. At these concentrations, cell viability did not decrease significantly compared with the control groups. Then, we seeded the FRTL-5 cells in 6-well plates (2 mL, 8×10^4 cells/well), cultured the plates overnight, and stimulated the cells with low PCB118 concentrations (0.025–25 nM). We observed the 6-well plates under a microscope and found that apoptosis began to appear approximately 72 h after PCB118 treatment; thus, we selected 72 h as the time point to perform the cell apoptosis assay. The cells were harvested 72h after PCB118 treatment and double-stained with annexin V-fluorescein isothiocyanate (FITC) and propidium iodide according to the manufacturer's protocol. Cell samples were quantitatively analyzed on a FACSVantage SE flow cytometer (BD Biosciences, USA) and apoptotic fractions were determined. Annexin V-FITC-positive cells reflected the relative proportion of apoptotic cells.

Quantitative real-time polymerase chain reaction (qRT-PCR) analysis of Akt, FoxO3a, and NIS

FRTL-5 cells were seeded in 6-well plates (2 mL, 16×10^4 cells/well), cultured overnight, and treated with low PCB118 concentrations (0.025–25 nM) for 24 h. At these concentrations, cells viability was not significantly decreased and showed no apoptotic difference compared with the control groups. Total RNA was isolated using RNAiso Plus (Takara, Japan) following the manufacturer's instructions and reverse transcribed to complementary DNAs using the Prime-Script RT Master Mix Kit (Takara). Quantitative RT-PCR was performed following a standard SYBR-Green PCR kit protocol on a Step One Plus system (Applied Biosystems, USA). β -actin was used as an endogenous control to normalize the total amount of mRNA in each sample. Relative expression levels of target genes were calculated using the $2^{-\Delta\Delta CT}$ method [32]. The

following primers were used: rat Akt, FoxO3a, NIS, and β -actin (all primers were synthesized by Takara); the primers are presented in [Table 1](#).

Western blotting analysis of Akt, p-Akt, FoxO3a, p-FoxO3a, and NIS

FRTL-5 cells were seeded in 6-well plates (2 mL, 15×10^4 cells/well) and treated as described above. After being cultured for 48 h with PCB118 or DMSO, proteins were extracted using a protein extraction kit (KeyGEN Biotech, China) according to the manufacturer's directions. Protein concentrations of the samples were measured using the Bio-Rad protein assay (Bio-Rad, USA). Then, 30 μ g of protein was denatured with 2% sodium dodecyl sulfate (SDS) and 50 mM dithiothreitol, loaded on an SDS-PAGE gel (10%), and transferred to a polyvinylidene fluoride membrane (Millipore, USA) using a standard protocol. Western blotting was performed as described previously [33], except for protein visualization, which was performed using an enhanced chemiluminescence reagent (Thermo, USA). The antibodies used in this procedure were Akt (1:1000 dilution), p-Akt (1:2000 dilution), FoxO3a (1:1000 dilution), glyceraldehyde 3-phosphate dehydrogenase (GAPDH, 1:1000 dilution), all purchased from Cell Signaling Technology (USA). p-FoxO3a(1:1000 dilution) was purchased from Abcam (USA), and NIS (1:250 dilution) was purchased from Bioss (USA), all primary antibodies were generated in rabbits. The secondary antibodies (goat anti-rabbit, 1:4000 dilution) were obtained from Bioworld (USA). GAPDH was used as the endogenous control to adjust the variation caused by protein loading.

Activation or suppression for the PI3K/Akt signaling pathway

The constitutively active Akt (CA-Akt) and dominant-negative Akt (DN-Akt) plasmids were constructed by Sunbio (Shanghai, China). FRTL-5 cells were seeded in 6-well plates to approximately 50% confluence and washed with 2 mL of warmed serum-free culture medium. Then, 2 mL of a premade plasmid/Lipofectamine mixture were added. This mixture was prepared by incubating 4 μ g of CA-Akt plasmid (DN-Akt or BC plasmid) with 10 μ L of Lipofectamine 2000 Transfection Reagent (Invitrogen, USA) and serum-free medium for 20 min at room temperature. The cells were randomly divided into three groups. The BC, CA-Akt, and DN-Akt groups consisted of cells treated with the BC, CA-Akt, and DN-Akt plasmids, respectively. The cells were incubated for 6 h before being refreshed with 2 mL of complete medium. Incubation of cells continued for 24 h, and then PCB118 (final concentration, 25 nM) or DMSO was added. After the cells were treated with PCB118 for 24 h, proteins were extracted and western blotting was performed to observe the effects of CA-Akt and DN-Akt on p-Akt, p-FoxO3a, and NIS levels in the FRTL-5 cells.

Table 1. Primers used for quantitative real-time PCR.

Primer	Primer sequences (5' to 3')	Genbank
Akt	Forward: GCCCAACACCTTCATCATCC	NM-033230.2
	Reverse: GTCTCCTCCTCCTGCCGTTT	
FoxO3a	Forward: TGCTAAGCAGGCCTCATCTCAA	NM-001106395
	Reverse: AGATGGCGTGGGAGTCACAA	
NIS	Forward: CCAAGAAGGCCAATCACA	NM-052983.2
	Reverse: CCGCTGCCTACTGAAATCT	
β -actin	Forward: GGAGATTACTGCCCTGGCTCCTA	NM-031144.3
	Reverse: GACTCATCGTACTCCTGCTTGCTG	

doi:10.1371/journal.pone.0120133.t001

Plasmid construction of FoxO3a promoter and NIS promoter

The NIS and FoxO3a gene sequences were searched using the NCBI Genome Database. Promoter prediction was conducted using McPromoter software, and then, the promoter sequences were verified using the dual luciferase reporter system. Finally, we determined the genomic sequences of the NIS promoter (5'-2235 to 5'-50 bp) and FoxO3a promoter (5'-2000 to 5'-20 bp). NIS promoter and FoxO3a promoter were amplified by PCR using the following primers: FoxO3a-forward: CCGAGCTCTTACGCGTTGTATTTACTCGTAAATGGGCC; FoxO3a-reverse: GATCGCAGATCTCGAGAGGGACGAGGCGGGAGG; NIS-forward: CCGAGCTCTTACGCGTCAACCCCACTGCAGTTTGTG; and NIS-reverse: GATCGCATCTCGAGGGAGACAGGTGACTCGGTGAG. The PCR product was subcloned into the luciferase reporter gene plasmid pGL3-basic (Invitrogen, USA) and termed FoxO3a-promoter-Luc or NIS-promoter-Luc. Wide-type pcDNA3-FoxO3a and BC plasmid were constructed by Invitrogen (USA). All inserts were confirmed by DNA sequencing.

Luciferase reporter assays of FoxO3a and NIS promoters

X-tremeGENE HP DNA Transfection Reagent (Roche, USA) was used to transfect a promoter/reporter gene into FRTL-5 cells. In brief, the cells were grown in 24-well plates to approximately 50% confluence and refreshed with 500 μ L of warmed (37°C) serum-free culture medium. Then, 50 μ L of a premade plasmid/transfection reagent mixture was added. This mixture contained serum-free culture medium, X-tremeGENE HP DNA Transfection Reagent, promoter-Luc plasmid, and renilla plasmid (the volume ratio of promoter plasmid and transfection reagent was 1:2, and the mass ratio of the promoter and renilla plasmids was 1:1000). PCB118 was added at different concentrations (0.025–25 nM) 24 h after transfection, and reporter activity was measured after 48 h. To determine the influence of FoxO3a on the NIS promoter, 0.15 μ g pcDNA3-FoxO3a or BC plasmid was co-transfected with 0.15 μ g NIS promoter plasmid. PCB118 at 25 nM or DMSO was added 24 h after transfection, and reporter activity was measured after 48 h. To measure luciferase activity, the cells were washed twice with 1 mL of 1 \times PBS, lysed with 100 μ L of 1 \times passive lysis buffer (Promega, USA), shaken for 15 min at room temperature, and pipetted repetitively for 30 times using a yellow-tip micropipette (200 μ L capacity). The lysate was then centrifuged at 12,000 rpm for 5 min at room temperature. Luciferase activity was analyzed using a Dual-Luciferase Reporter Assay System (Promega) according to the manufacturer's protocol using a Glomax Luminometer (Promega). Data represented the mean \pm standard deviation (SD) of triplicate samples and were expressed as relative values.

FoxO3a-specific small interfering RNA(siRNA)analysis

To transiently knockdown the expression of the genes of interest, we used FoxO3a-targeting siRNA. FRTL-5 cells were seeded in 6-well plates to approximately 50% confluence and washed with 2 mL of warmed serum-free culture medium. Then, 2 mL of a premade siRNA/Lipofectamine mixture was added. This mixture was prepared by incubating 5 μ L of siRNA with 5 μ L of Lipofectamine 2000 Transfection Reagent (Invitrogen) and 500 μ L of serum-free medium for 20 min at room temperature, and then diluting it with 1.5 mL of serum-free medium. The cells were randomly divided into two groups. The negative control (NC) group consisted of cells treated with non-target siRNA. The FoxO3a-siRNA group consisted of cells treated with FoxO3a siRNA (target siRNA). The cells were incubated for 6 h before being placed in serum-free medium with 2 mL of complete medium. The cells were incubated for 24 h, and then PCB118 (final concentration, 25 nM) or DMSO was added. After the cells were treated with PCB118 or DMSO for 48 h, proteins were extracted and western blotting was performed to

observe the effects of siRNA on FoxO3a, p-FoxO3a, and NIS levels in the FRTL-5 cells. Both FoxO3a and NC siRNAs were synthesized by Invitrogen (USA).

Statistical analysis

Data are presented as the mean \pm SD of at least three independent experiments. The SPSS 13.0 statistical package (SPSS Inc., Chicago, IL, USA) was used to perform paired *t*-tests and one-way analysis of variance (ANOVA), the least significant difference (LSD) was used to perform post-hoc analysis after ANOVA, and a *p* value of <0.05 was considered significant.

Results

PCB118 inhibited cell viability in a concentration and time-dependent manners

As shown in [Fig. 2A](#), cells were stimulated with media culture, DMSO, or different concentrations of PCB118 (0.025–25000 nM) for 24h, 48h, and 72 h. From 24 h to 72 h, no significant difference was observed between the BC and DMSO groups ($p > 0.05$). Within 24 h, no evident difference in cell viability was observed between PCB118 (0.025–25000 nM)-treated groups and the DMSO control group ($p > 0.05$), and no significant difference was observed between each PCB118-treated group ($p > 0.05$). However, relatively higher PCB118 concentrations (250–25000 nM) could significantly decrease cell viability compared with the DMSO control group or low PCB118 concentrations (0.025, 0.25, 2.5, 25nM)-treated groups ($p < 0.05$) when the incubation time was extended to 48 and 72 h. Thus, PCB118 could suppress cell viability in a concentration- and time-dependent manner.

Therefore, low PCB118 concentrations (0.025, 0.25, 2.5, and 25 nM) were selected in cell apoptosis experiment in FRTL-5 cells.

Low PCB118 concentrations did not induce cell apoptosis

The cell apoptosis assay was performed to determine whether relatively low PCB118 concentrations (0.025–25 nM) could induce cell apoptosis. As shown in [Fig. 2B](#), no significant difference was observed in the cell apoptosis rates of PCB118-treated and DMSO control groups ($p > 0.05$), and the difference between each PCB118-treated group was also not significant ($p > 0.05$).

Because our results indicated that PCB118 at high concentrations (250–25000 nM) is an effective inhibitor of FRTL-5 cell viability and PCB118 at low concentrations (0.025–25 nM) does not induce cell apoptosis or influence cell viability, we selected PCB118 concentrations of 0.025–25 nM for subsequent experiments.

PCB118 treatment decreases NIS expression

To investigate whether PCB118 had an effect on NIS expression, western blotting, qRT-PCR, and luciferase reporter assays of the NIS promoter were performed. As shown in [Fig. 3](#), after treatment with various concentrations of PCB118 for 24 h (for qRT-PCR analysis) or 48 h (for Western blot analysis and luciferase reporter assays), both protein ([Fig. 3A, B](#)) and mRNA levels ([Fig. 3C](#)) of NIS decreased significantly ($p < 0.05$) after treatment with low PCB118 concentrations (0.025–25 nM) compared with the DMSO control group. Similar to the mRNA and protein results, PCB118 suppressed NIS promoter activity significantly ($p < 0.05$; [Fig. 3D](#)). However, no significant difference was observed between each PCB118-treated group ($p > 0.05$). Altogether, these results suggest that PCB118 down-regulates NIS expression at

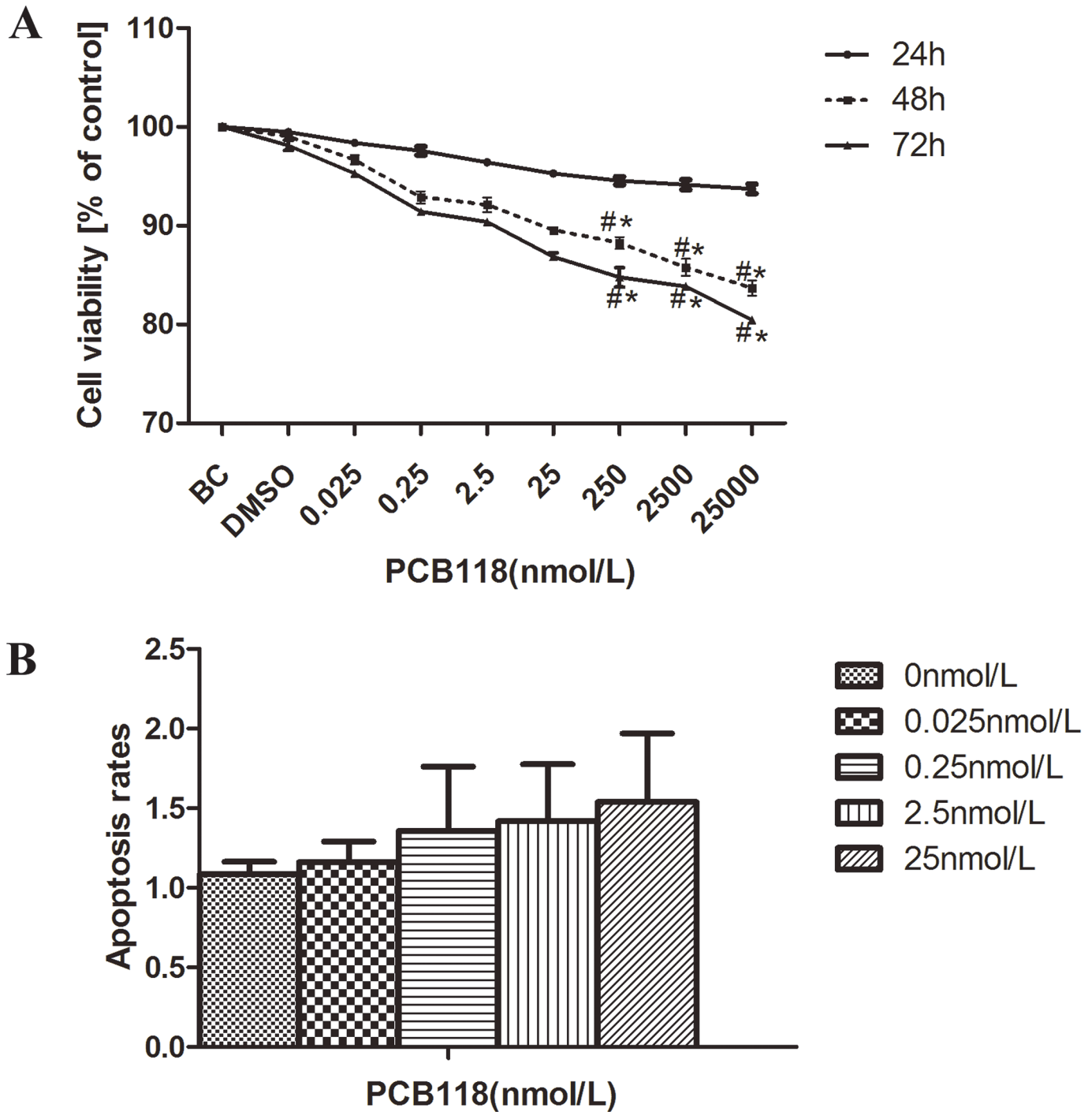


Fig 2. Effect of PCB118 on FRTL-5 cell viability and apoptosis. Cells were treated with PCB118 at different concentrations (0.025–25000 nM in the Cell Counting Kit-8 (CCK8) assay and 0.025–25 nM in the apoptosis assay). The viability was measured using the CCK-8 assay (A). The apoptosis rate was measured using a FACS Vantage SE flow cytometer (B). Data are presented as the mean ± SD of three independent experiments. * $p < 0.05$, compared with the DMSO control group. # $p < 0.05$, compared with the low PCB118-treated groups (0.025, 0.25, 2.5, and 25 nM).

doi:10.1371/journal.pone.0120133.g002

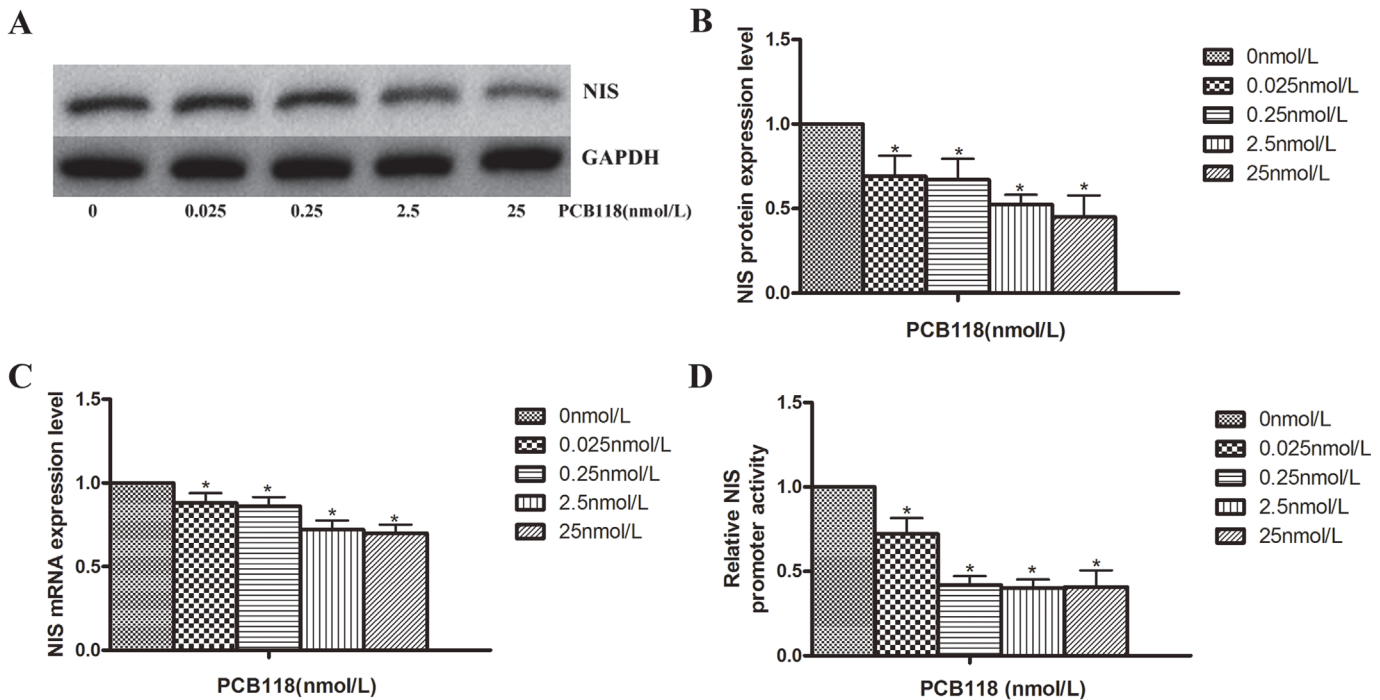


Fig 3. Exposure of FRTL-5 cells to PCB118 results in the down-regulation of NIS expression. Cells were treated with DMSO or various concentrations of PCB118 (0.025–25 nM) for 24 or 48 h. Whole cell lysates were analyzed by western blotting using antibodies recognizing NIS (A and B). Total RNA was isolated for qRT-PCR of NIS (C), and the FRTL-5 cells were harvested for the measurement of NIS promoter activity (D). Results show sections of blots from one experiment of the three that yielded similar results (A) or represented the mean \pm SD of three independent experiments (B, C, and D). GAPDH served as the loading control in western blotting. * $p < 0.05$, compared with the DMSO control group. The relative ratio of target mRNA/ β -actin, target protein/GAPDH and promoter activity in solvent control group was set as 1.

doi:10.1371/journal.pone.0120133.g003

both the mRNA and protein levels. Furthermore, such results were observed occurred at the transcriptional level.

FoxO3a down-regulates NIS expression

In our study, we found that the p-FoxO3a protein expression level increased (Fig. 4A, B) and FoxO3a promoter activity was enhanced after PCB118 treatment (Fig. 4D). Thus, we hypothesized that FoxO3a may play a role in regulating NIS expression. To examine whether FoxO3a regulated NIS expression, we designed siRNAs targeted to FoxO3a. Western blotting revealed that FoxO3a was efficiently downregulated by targeted siRNA in both the DMSO control group and 25 nM PCB118-treated groups ($p < 0.05$; Fig. 5A, B). The downregulation of FoxO3a resulted in decreased FoxO3a phosphorylation on stimulation with PCB118; thus, the protein expression levels of p-FoxO3a were also decreased by siRNA in the PCB118-treated group ($p < 0.05$; Fig. 5A and 5B). Compared with the PCB118-treated NC group and the DMSO control group, siRNA-induced FoxO3a downregulation led to an increase in NIS protein levels in the 25 nM PCB118-treated group ($p < 0.05$; Fig. 5A and B). To further study whether FoxO3a regulated NIS expression, the pcDNA3-FoxO3a or BC plasmid was co-transfected with the NIS promoter plasmid into FRTL-5 cells. As shown in Fig. 5C, after 48 h, FoxO3a over-expression led to significant reduction in NIS promoter activity ($p < 0.05$) in PCB118-treated group when compared to the BC group or DMSO control group ($p < 0.05$). These results may indicate that FoxO3a plays an important role in the down-regulation of NIS expression in PCB118-treated FRTL-5 cells.

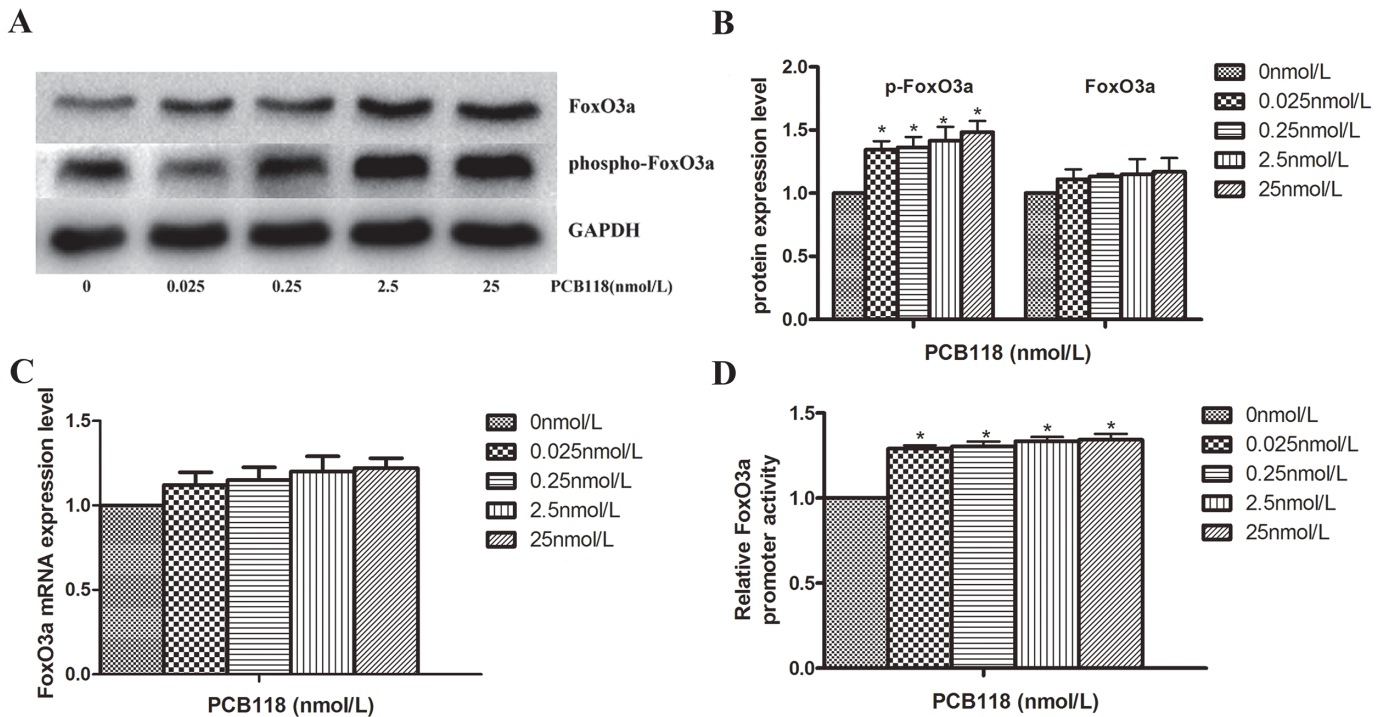


Fig 4. Exposure of FRTL-5 cells to PCB118 results in the up-regulation of FoxO3a or p-FoxO3a expression. Cells were treated with DMSO or various concentrations of PCB118 (0.025–25 nM) for 24 or 48 h. Whole cell lysates were analyzed by western blotting using antibodies recognizing FoxO3a and p-FoxO3a. GAPDH served as the loading control (A and B). Total RNA was isolated for qRT-PCR of FoxO3a (C), and the PCB118-treated FRTL-5 cells were harvested for the measurement of FoxO3a promoter activity (D). Results show sections of blots from one experiment of the three that yielded similar results (A) or represent the mean \pm SD of three independent experiments (B, C, and D). GAPDH served as the loading control in western blotting. * $p < 0.05$, compared with the DMSO control group. The relative ratio of target mRNA/ β -actin, target protein/GAPDH and promoter activity in solvent control group was set as 1.

doi:10.1371/journal.pone.0120133.g004

PCB118-induced reduction in NIS expression depends on the activation of the PI3K/Akt/FoxO3a signaling pathway

Fig. 6 shows that Akt and p-Akt protein levels and Akt mRNA levels increased significantly in the PCB118-treated groups compared with the DMSO control group ($p < 0.05$; Fig. 6 A, B, C). This result showed that the PI3K/Akt signaling pathway was activated in FRTL-5 cells after exposure to PCB118. To verify whether the activation of the PI3K/Akt signaling pathway could down-regulate NIS expression, the CA-Akt or DN-Akt plasmid was transfected into FRTL-5 cells. The cells were harvested for western blotting, and the variation in the p-Akt, p-FoxO3a, and NIS protein levels was examined. Compared to the DMSO control group and PCB118-treated BC (blank plasmid control) group respectively, the expression level of p-Akt and p-FoxO3a increased significantly and NIS expression decreased dramatically in 25nM PCB118-treated group when transfected with CA-Akt plasmid ($p < 0.05$), whereas the opposite results were obtained in PCB118-treated group transfected with DN-Akt plasmid ($p < 0.05$; Fig. 6D, E). Therefore, we suggest that PCB118 down-regulates NIS expression, perhaps through the activation of the PI3K/Akt/FoxO3a signaling pathway.

Discussion

In a previous study, we demonstrated that persistent exposure to low PCB118 concentrations could severely damage thyroidal structure, dramatically decreasing the concentration of serum thyroid hormones. Furthermore, pivotal gene expression such as NIS and thyroglobulin, which

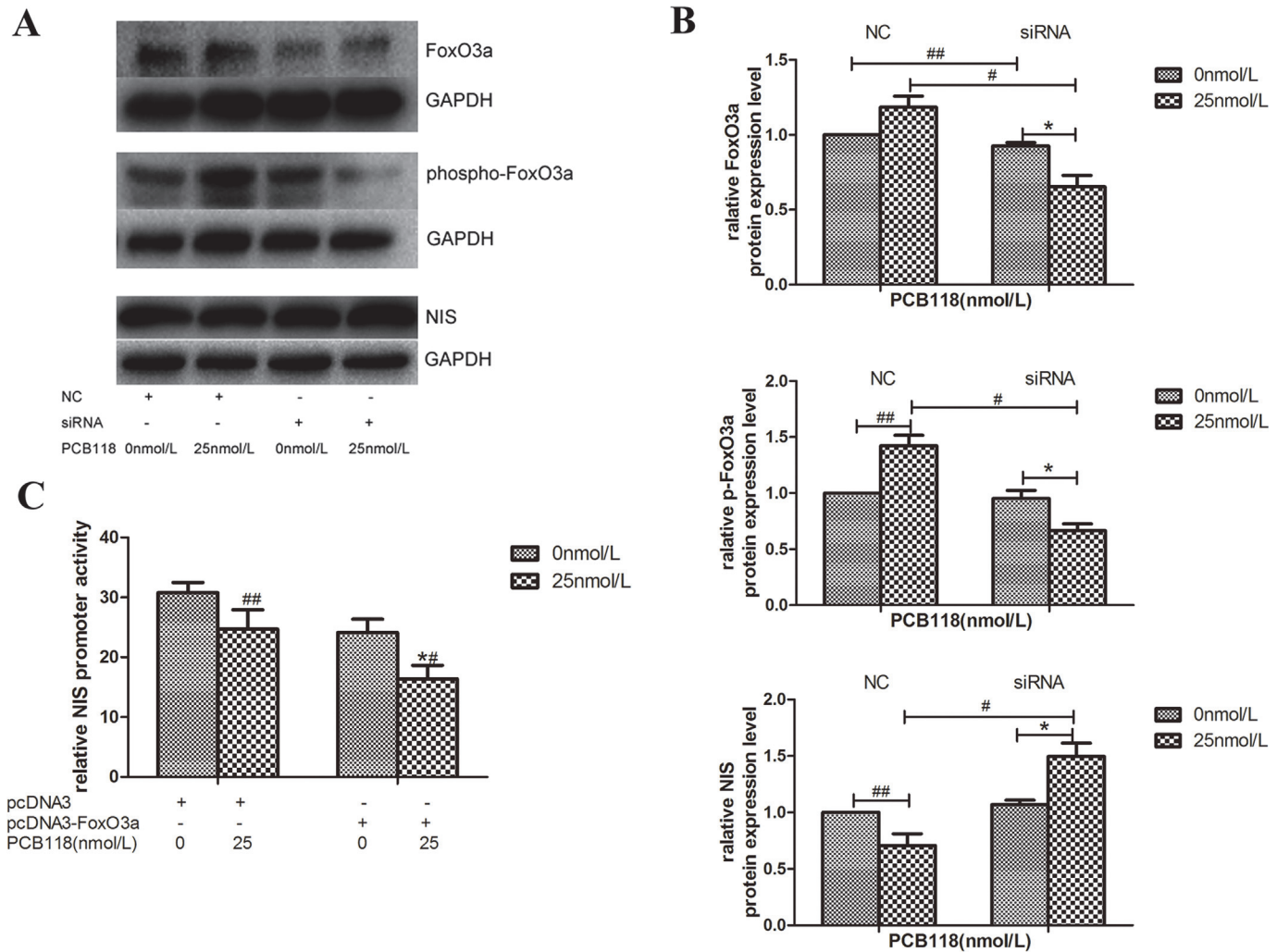


Fig 5. FoxO3a plays a role in the down-regulation of NIS expression in PCB118-treated FRTL-5 cells. FoxO3a was knocked down by FoxO3a-siRNA in FRTL-5 cells, and the cells were treated with PCB118 at 25 nM. Whole cell lysates were analyzed by western blotting using antibodies recognizing FoxO3a, p-FoxO3a, and NIS (A and B). FoxO3a over-expression was induced by the pcDNA3-FoxO3a plasmid, and the cells were harvested for the measurement of NIS promoter activity (C). Results show sections of blots from one experiment of the three that yielded similar results (A) or represent the mean \pm SD of three independent experiments (B and C). GAPDH served as the loading control in western blotting. * $p < 0.05$, compared with the DMSO control group transfected with siRNA or the pcDNA3-FoxO3a plasmid; # $p < 0.05$, compared with the 25 nM PCB118-treated group transfected with the NC or pcDNA3 plasmid; ## $p < 0.05$, compared with the DMSO control group transfected with the NC or pcDNA3 plasmid. The relative ratio of target protein/GAPDH and promoter activity in solvent control group was set as 1.

doi:10.1371/journal.pone.0120133.g005

determine the synthesis and secretion of thyroid hormones, was remarkably decreased in Wistar rats [6]. In the present study, we continued exploring the molecular mechanisms of FRTL-5 dysfunction related to low concentrations of PCB118 exposure in vitro.

PCBs consist of a series of 209 individual congeners according to the number and position of the substituent chlorine on a biphenyl structure and can be classified into three types of inducers: 2, 3, 7, 8-tetrachlorodibenzo-*p*-dioxin (TCDD)-type, phenobarbital (PB)-type, and mixed (TCDD/PB)-type inducers. 3,3',4,4',5-Pentachlorobiphenyl (PCB126) and 2,2',4,4',5,5'-hexachlorobiphenyls (PCB153) are representatives of the TCDD- and PB-type inducers, respectively [34]. In contrast, PCB118 is considered a mixed (TCDD/PB)-type inducer [34] (McFarland and Clarke 1989) and shares the properties of both TCDD- and PB-type inducers. In addition, PCB118 is one of the most persistent PCB congeners and has been found in human tissues and

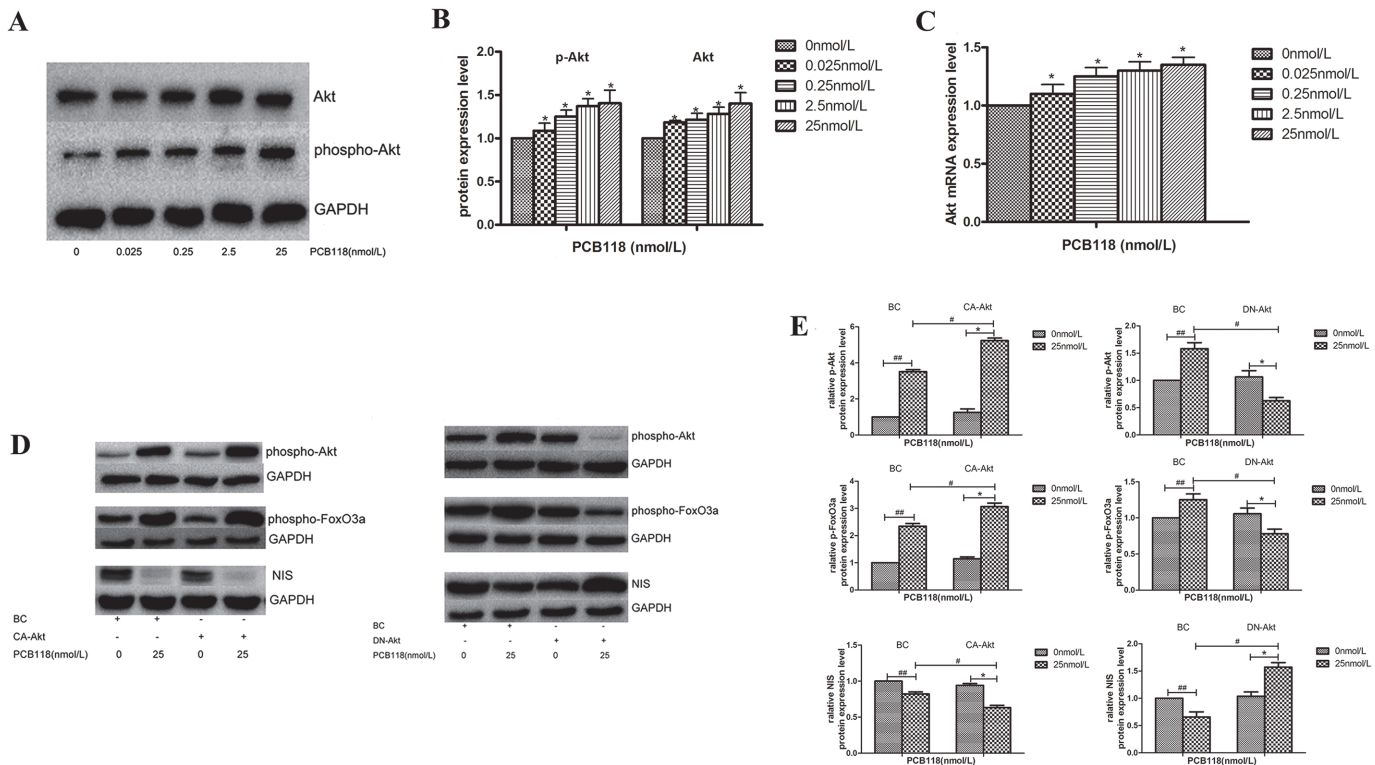


Fig 6. Akt pathway was activated in PCB118-treated FRTL-5 cells. Cells were treated with DMSO or various concentrations of PCB118 (0.025–25 nM) for 24 or 48 h. Whole cell lysates were analyzed by western blotting using antibodies recognizing Akt and p-Akt (A and B). Total RNA was isolated for qRT-PCR of Akt (C). Up-regulation of Akt expression was induced by CA-Akt and down-regulation was induced by DN-Akt in FRTL-5 cells. After treatment with 25 nM PCB118 for 48 h, whole cell lysates were analyzed by western blotting using antibodies recognizing p-Akt, p-FoxO3a, and NIS (D and E). Results show sections of blots from one experiment of the three that yielded similar results (A and D) or represent the mean \pm SD of three independent experiments (B, C, and E). GAPDH served as the loading control in western blotting. * $p < 0.05$, compared with the DMSO control group (Fig. 6B, C) * $p < 0.05$, compared with the DMSO control group transfected with the CA-Akt or DN-Akt plasmid (Fig. 6E); # $p < 0.05$, compared with the 25 nM PCB118-treated group transfected with the BC plasmid; ## $p < 0.05$, compared with the DMSO control group transfected with the BC plasmid. The relative ratio of target mRNA/ β -actin and target protein/GAPDH in solvent control group was set as 1.

doi:10.1371/journal.pone.0120133.g006

detected in human breast milk [35]. It is also one of the nine PCB congeners most strongly linked to thyroid dysfunction [36], and its contamination is widespread in water and soil and among the aquatic organisms of the Yangtze River Delta region of China. We selected PCB118 as the representative contaminant for the study.

In our previous *in vivo* study, we found significant deterioration of the thyroid structure and function even at a minimal dosage of 10 μ g/kg/day (approximately 6 \times 10⁴ nM per day)[6], and previous study indicated that serum concentration of PCBs reach approximately 3 \times 10³ nM in people exposed to PCBs [37]. These concentrations were out of the range of concentrations used in the *in vitro* experiment; however, the *in vivo* and *in vitro* experiments are different; thus, we referred to PCB concentrations from other *in vitro* studies [38,39]. Moreover, the concentration of our PCB118 stock solution was 25 mM to facilitate convenient dilutions into different concentrations, and we adopted concentrations of 0.025–25,000 nM to perform the CCK8 assay.

In the first step of the CCK-8 cell viability test, it was found that PCB118 inhibited cell viability in a concentration- and time-dependent manner at concentrations ranging from 0.025 nM to 25000 nM. Significant deterioration of cell viability was revealed at relatively high concentrations (250–25000 nM). According to this result, we selected the concentration range of

0.025–25 nM as the low PCB118 concentrations in subsequent research. It was found that when PCB118 was used at concentrations of 0.025–25 nM, it did not influence either cell viability or cell apoptosis. However, series variations in genes and proteins were observed, such as NIS, Akt, p-Akt, and p-FoxO3a. This may indicate that the damage caused by low concentrations of PCB118 to thyroid-specific genes was more remarkable than the influence of PCB118 on FRTL-5 cell viability.

On the other hand, such low PCB118 concentrations (0.025–25 nM) was far below the concentrations used in some other previous studies related to the effect of PCB exposure on thyroid and neuroendocrine systems [40–42]. However, these concentrations in our study were very similar to those of 1 pM to 1 μM used by Rankouhi et al. in primary hepatocytes of fish, which had little or no influence on cell viability [43]. The difference in these detections may be caused by different types of PCBs, the duration of contaminant stimulation, or distinct characteristics of cells in each experiment, and the observed endpoints of respective studies.

Our existing results also found that at 0.025–25 nM of PCB118 could significantly inhibit both mRNA and protein expression levels of NIS, and NIS promoter activity was suppressed; this suggested that chronic PCB118 exposure posed a significant risk for thyroid dysfunction. The above mentioned findings are remarkably consistent with those of a previous study in which NIS gene activity was significantly down-regulated at 306 nM PCB126 [44] and our previous research *in vivo* that PCB118 could result in progressively lower FT3, FT4 and TSH concentrations in serum, led to histopathological deterioration of the thyroid (such as follicular hyperplasia and expansion, shedding of epithelial cells and fibrinoid necrosis), and cause significant decreases in NIS mRNA expression levels [6]. Other series of studies also indicated that PCBs could inhibit the process of thyroid hormone production [8,45], which may result from the reduction in NIS expression, yet the specific mechanism is unknown. It has been reported that TSH can down-regulate NIS expression through the Gβγ/PI3K/Akt pathway [46]. Moreover, Kogai et al. illustrated that the activation of the PI3K signaling pathway in TSH-stimulated thyroid cells causes a reduction in NIS expression at the transcription level [47]. It was also found that inhibition of the PI3K/Akt signaling pathway increased the expression of NIS mRNA and protein [48], as well as up-regulated the activation of the NIS promoter [49]. In our study, constitutive activation of Akt enhanced the decrease in PCB118-induced NIS expression level, whereas dominant-negative Akt was sufficient to reverse the decrease in PCB118-induced NIS expression level. These results suggest that the PI3K/Akt pathway was activated in PCB118-treated FRTL-5 cells. It is well established that the PI3K/Akt pathway is crucial for cellular processes [50]. Following its phosphorylation, Akt activates a number of downstream targets. However, as one of the most important downstream targets the PI3K/Akt pathway [18], whether FoxO3a plays a key role in regulating NIS expression is still unknown. In our study, in PCB118-treated FRTL-5 cells, the PI3K/Akt pathway was activated, and FoxO3a was phosphorylated by Akt, leading to its translocation to the cytoplasm and an elevation of p-FoxO3a. This signifies that at low PCB concentrations, total FoxO3a did not appear to significantly change, whereas the proportion of p-FoxO3a increased. Meanwhile, we also found the increased p-FoxO3a expression level could be reversed by FoxO3a-siRNA, simultaneously, accompanied with the increased NIS expression level. Moreover, the NIS promoter activity was notably reduced when overexpressing of FoxO3a. The aforementioned results suggested that FoxO3a may act as a transcription factor that regulates NIS expression.

In the study, we discovered that PCB118 down-regulates NIS expression in FRTL-5 cells, at least in part, through activated of PI3K/Akt pathway and enhanced p-FoxO3a which revealed the inactivated FoxO3a increased. Hence, our study indicates that the molecular mechanism of dysfunction of FRTL-5 thyrocyte cells induced by PCB118 involves the PI3K/Akt/FoxO3a pathway. This finding has advanced our understanding of the role of PCB118 in thyrocytes

and provides a new concept that may prove effective in blocking the damage caused by PCBs to the human body. However, the role of the DNA binding site of FoxO3a in or around the NIS promoter area remains unclear. This is the goal of our further research using the electrophoretic mobility shift assay and chromatin immunoprecipitation.

Acknowledgments

The authors thank Dr. Zheng Xuqin for her kindly providing of FRTL-5 cells.

Author Contributions

Conceived and designed the experiments: HY HHC HWG WL JMT BJX MNS GXD LJ DC XQZ YD. Performed the experiments: HY HHC HWG WL JMT BJX MNS GXD LJ DC XQZ YD. Analyzed the data: HY HHC HWG WL JMT BJX MNS GXD LJ DC XQZ YD. Contributed reagents/materials/analysis tools: HY HHC HWG WL JMT BJX MNS GXD LJ DC XQZ YD. Wrote the paper: HY HHC HWG WL JMT BJX MNS GXD LJ DC XQZ YD.

References

1. Arnold DL, Bryce F, McGuire PF, Stapley R, Tanner JR, Wrenshall E, et al. Toxicological consequences of aroclor 1254 ingestion by female rhesus (*Macaca mulatta*) monkeys. Part 2. Reproduction and infant findings. *Fd Chem Toxicol.* 1995; 33: 457–474.
2. Golden R, Kimbrough R. Weight of evidence evaluation of potential human cancer risks from exposure to polychlorinated biphenyls: an update based on studies published since 2003. *Crit Rev Toxicol.* 2009; 39: 299–331. doi: [10.1080/10408440802291521](https://doi.org/10.1080/10408440802291521) PMID: [19514916](https://pubmed.ncbi.nlm.nih.gov/19514916/)
3. Portigal CL, Cowell SP, Fedoruk MN, Butler CM, Rennie PS, Nelson CC. Polychlorinated biphenyls interfere with androgen-induced transcriptional activation and hormone binding. *Toxicol Appl Pharmacol.* 2002; 179: 185–194. PMID: [11906248](https://pubmed.ncbi.nlm.nih.gov/11906248/)
4. Zhao G, Wang Z, Zhou H, Zhao Q. Burdens of PBBs, PBDEs, and PCBs in tissues of the cancer patients in the e-waste disassembly sites in Zhejiang, China. *Sci Total Environ.* 2009; 407: 4831–4837. doi: [10.1016/j.scitotenv.2009.05.031](https://doi.org/10.1016/j.scitotenv.2009.05.031) PMID: [19539352](https://pubmed.ncbi.nlm.nih.gov/19539352/)
5. Rolland RM. A review of chemically induced alterations in thyroid and vitamin A status from field studies of wildlife and fish. *Journal of Wildlife Diseases.* 2000; 36: 615–635. PMID: [11085423](https://pubmed.ncbi.nlm.nih.gov/11085423/)
6. Tang JM, Li W, Xie YC, Guo HW, Cheng P, Chen HH, et al. Morphological and functional deterioration of the rat thyroid following chronic exposure to low-dose PCB118. *Exp Toxicol Pathol.* 2013; 65: 989–994. doi: [10.1016/j.etp.2013.02.001](https://doi.org/10.1016/j.etp.2013.02.001) PMID: [23557935](https://pubmed.ncbi.nlm.nih.gov/23557935/)
7. Ishihara A, Sawatsubashi S, Yamauchi K. Endocrine disrupting chemicals: interference of thyroid hormone binding to transthyretins and to thyroid hormone receptors. *Mol Cell Endocrinol.* 2003; 199: 105–117. PMID: [12581883](https://pubmed.ncbi.nlm.nih.gov/12581883/)
8. Boas M, Feldt-Rasmussen U, Skakkebaek NE, Main KM. Environmental chemicals and thyroid function. *Eur J Endocrinol.* 2006; 154: 599–611. PMID: [16645005](https://pubmed.ncbi.nlm.nih.gov/16645005/)
9. Brown SB, Adams BA, Cyr DG, Eales JG. Contaminant effects on the teleost fish thyroid. *Environ Toxicol Chem.* 2004; 23: 1680–1701. PMID: [15230321](https://pubmed.ncbi.nlm.nih.gov/15230321/)
10. Dohan O, De la Vieja A, Paroder V, Riedel C, Artani M, Reed M, et al. The sodium/iodide symporter (NIS): characterization, regulation, and medical significance. *Endocr Rev.* 2003; 24: 48–77. PMID: [12588808](https://pubmed.ncbi.nlm.nih.gov/12588808/)
11. Kogai T, Taki K, Brent GA. Enhancement of sodium/iodide symporter expression in thyroid and breast cancer. *Endocr Relat Cancer.* 2006; 13: 797–826. PMID: [16954431](https://pubmed.ncbi.nlm.nih.gov/16954431/)
12. Serrano-Nascimento C, da Silva Teixeira S, Nicola JP, Nachbar RT, Masini-Repiso AM, Nunes MT. The acute inhibitory effect of iodide excess on sodium/iodide symporter expression and activity involves the PI3K/Akt signaling pathway. *Endocrinology.* 2014; 155: 1145–1156. doi: [10.1210/en.2013-1665](https://doi.org/10.1210/en.2013-1665) PMID: [24424051](https://pubmed.ncbi.nlm.nih.gov/24424051/)
13. Bauer TM, Patel MR, Infante JR. Targeting PI3 kinase in cancer. *Pharmacol Ther.* 2014; 8. Available: <http://dx.doi.org/10.1016/j.pharmthera.2014.09.006>.
14. Dal Col J, Zancai P, Terrin L, Guidoboni M, Ponzoni M, Pavan A, et al. Distinct functional significance of Akt and mTOR constitutive activation in mantle cell lymphoma. *Blood.* 2008; 111: 5142–5151. doi: [10.1182/blood-2007-07-103481](https://doi.org/10.1182/blood-2007-07-103481) PMID: [18339899](https://pubmed.ncbi.nlm.nih.gov/18339899/)

15. Laia Rosich AM, Xargay-Torrent S, López-Guerra M, Roldán J, Aymerich M, Salaverria I, et al. Dual PI3K_mTOR inhibition is required to effectively impair microenvironment survival signals in mantle cell lymphoma. *Oncotarget*. 2014; 5:6788–6800. PMID: [25216518](#)
16. Rodon J, Dienstmann R, Serra V, Tabernero J. Development of PI3K inhibitors: lessons learned from early clinical trials. *Nat Rev Clin Oncol*. 2013; 10: 143–153. doi: [10.1038/nrclinonc.2013.10](#) PMID: [23400000](#)
17. Manning BD, Cantley LC. AKT/PKB signaling: navigating downstream. *Cell*. 2007; 129: 1261–1274. PMID: [17604717](#)
18. Brunet A, Bonni A, Zigmond MJ, Lin MZ, Juo P, Hu LS, et al. Akt promotes cell survival by phosphorylating and inhibiting a Forkhead transcription factor. *Cell*. 1999; 96: 857–868. PMID: [10102273](#)
19. Medema RH, Kops GJ, Bos JL, Burgering BM. AFX-like Forkhead transcription factors mediate cell-cycle regulation by Ras and PKB through p27kip1. *Nature*. 2000; 404: 782–787. PMID: [10783894](#)
20. Luo X, Puig O, Hyu J, Bohmann D, Jasper H. Foxo and Fos regulate the decision between cell death and survival in response to UV irradiation. *Embo J*. 2007; 26: 380–390. PMID: [17183370](#)
21. Olmos Y, Valle I, Borniquel S, Tierrez A, Soria E, Lamas S, et al. Mutual dependence of Foxo3a and PGC-1alpha in the induction of oxidative stress genes. *J Biol Chem*. 2009; 284: 14476–14484. doi: [10.1074/jbc.M807397200](#) PMID: [19324885](#)
22. Kops GJ, Dansen TB, Polderman PE, Saarloos I, Wirtz KW, Coffey PJ, et al. Forkhead transcription factor FOXO3a protects quiescent cells from oxidative stress. *Nature*. 2002; 419: 316–321. PMID: [12239572](#)
23. Van Der Heide LP, Hoekman MF, Smidt MP. The ins and outs of FoxO shuttling: mechanisms of FoxO translocation and transcriptional regulation. *Biochem J*. 2004; 380: 297–309. PMID: [15005655](#)
24. Guerrieri F, Piconese S, Lacoste C, Schinzari V, Testoni B, Valogne Y, et al. The sodium/iodide symporter NIS is a transcriptional target of the p53-family members in liver cancer cells. *Cell Death Dis*. 2013; 4: e807. doi: [10.1038/cddis.2013.302](#) PMID: [24052075](#)
25. Sastre-Perona A, Santisteban P. Wnt-Independent Role of beta-Catenin in Thyroid Cell Proliferation and Differentiation. *Mol Endocrinol*. 2014; 28: 681–695. doi: [10.1210/me.2013-1377](#) PMID: [24645679](#)
26. Medina DL, Santisteban P. Thyrotropin-dependent proliferation of in vitro rat thyroid cell systems. *Eur J Endocrinol*. 2000; 143: 161–178. PMID: [10913934](#)
27. Weidinger C, Krause K, Mueller K, Klagge A, Fuhrer D. FOXO3 is inhibited by oncogenic PI3K/Akt signaling but can be reactivated by the NSAID sulindac sulfide. *J Clin Endocrinol Metab*. 2011; 96: E1361–E1371. doi: [10.1210/jc.2010-2453](#) PMID: [21752881](#)
28. Zheng XQ, Cui D, Xu SH, Brabant G, Derwahl M. Doxorubicin fails to eradicate cancer stem cells derived from anaplastic thyroid carcinoma cells: Characterization of resistant cells. *International Journal of Oncology*. 2010; 37:307–315. PMID: [20596658](#)
29. Lan L, Cui D, Nowka K, Derwahl M. Stem cells derived from goiters in adults form spheres in response to intense growth stimulation and require thyrotropin for differentiation into thyrocytes. *J Clin Endocrinol Metab*. 2007; 92: 3681–3688. PMID: [17609303](#)
30. Kawashima A, Tanigawa K, Akama T, Wu H, Sue M, Yoshihara A, et al. Fragments of genomic DNA released by injured cells activate innate immunity and suppress endocrine function in the thyroid. *Endocrinology*. 2011; 152: 1702–1712. doi: [10.1210/en.2010-1132](#) PMID: [21303947](#)
31. Liu X, Zhang B, Guo Y, Liang Q, Wu C, Wu L, et al. Down-regulation of AP-4 inhibits proliferation, induces cell cycle arrest and promotes apoptosis in human gastric cancer cells. *PLOS ONE*. 2012; 7: e37096. doi: [10.1371/journal.pone.0037096](#) PMID: [22615908](#)
32. Livak KJ, Schmittgen TD. Analysis of relative gene expression data using real-time quantitative PCR and the 2⁻(Delta Delta C (T)) Method. *Methods*. 2001; 25: 402–408. PMID: [11846609](#)
33. Ohashi E, Miyajima N, Nakagawa T, Takahashi T, Kagechika H, Mochizuki M, et al. Retinoids induce growth inhibition and apoptosis in mast cell tumor cell lines. *J Vet Med Sci*. 2006; 68: 797–802. PMID: [16953078](#)
34. McFarland VA, Clarke JU. Environmental occurrence, abundance, and potential toxicity of polychlorinated biphenyl congeners: considerations for a congener-specific analysis. *Environ Health Perspect*. 1989; 81:225–239. PMID: [2503374](#)
35. Tarkowski S. Environmental health in Europe. A WHO perspective. *Int J Occup Med Environ Health*. 1996; 9: 1–6. PMID: [8776147](#)
36. Bloom MS, Weiner JM, Vena JE, Beehler GP. Exploring associations between serum levels of select organochlorines and thyroxine in a sample of New York state sportsmen: the New York State Angler Cohort Study. *Environ Res*. 2003; 93: 52–66. PMID: [12865048](#)

37. Wassermann M, Wassermann D, Cucos S, Miller HJ. World PCBs map: storage and effects in man and his biologic environment in the 1970s. *Ann N Y Acad Sci.* 1979; 320: 69–124. PMID: [110205](#)
38. Al-Anati L, Hogberg J, Stenius U. Non-dioxin-like PCBs interact with benzo[a]pyrene-induced p53-responses and inhibit apoptosis. *Toxicol Appl Pharmacol.* 2010; 249: 166–177. doi: [10.1016/j.taap.2010.09.004](#) PMID: [20840854](#)
39. Venkatesha VA, Kalen AL, Sarsour EH, Goswami PC. PCB-153 exposure coordinates cell cycle progression and cellular metabolism in human mammary epithelial cells. *Toxicol Lett.* 2010; 196: 110–116. doi: [10.1016/j.toxlet.2010.04.005](#) PMID: [20394812](#)
40. Howard A. Polychlorinated biphenyls induce caspase-dependent cell death in cultured embryonic rat hippocampal but not cortical neurons via activation of the ryanodine receptor. *Toxicology and Applied Pharmacology.* 2003; 190: 72–86. PMID: [12831785](#)
41. Merritt RL, Foran CM. Influence of persistent contaminants and steroid hormones on glioblastoma cell growth. *J Toxicol Environ Health A.* 2007; 70: 19–27. PMID: [17162496](#)
42. Sanchez-Alonso JA, Lopez-Aparicio P, Recio MN, Perez-Albarsanz MA. Apoptosis-mediated neurotoxic potential of a planar (PCB 77) and a nonplanar (PCB 153) polychlorinated biphenyl congeners in neuronal cell cultures. *Toxicol Lett.* 2003; 144: 337–349. PMID: [12927351](#)
43. Rankouhi TR, Sanderson JT, van Holsteijn I, van Leeuwen C, Vethaak AD, van den Berg M. Effects of natural and synthetic estrogens and various environmental contaminants on vitellogenesis in fish primary hepatocytes: comparison of bream (*Abramis brama*) and carp (*Cyprinus carpio*). *Toxicol Sci.* 2004; 81: 90–102. PMID: [15159526](#)
44. Pocar P, Klonisch T, Brandsch C, Eder K, Frohlich C, Hoang-Vu C, et al. AhR-agonist-induced transcriptional changes of genes involved in thyroid function in primary porcine thyrocytes. *Toxicol Sci.* 2006; 89: 408–414. PMID: [16291828](#)
45. Kato Y, Ikushiro S, Haraguchi K, Yamazaki T, Ito Y, Suzuki H, et al. A possible mechanism for decrease in serum thyroxine level by polychlorinated biphenyls in Wistar and Gunn rats. *Toxicol Sci.* 2004; 81: 309–315. PMID: [15254343](#)
46. Zaballos MA, Garcia B, Santisteban P. Gbetagamma dimers released in response to thyrotropin activate phosphoinositide 3-kinase and regulate gene expression in thyroid cells. *Mol Endocrinol.* 2008; 22: 1183–1199. doi: [10.1210/me.2007-0093](#) PMID: [18202153](#)
47. Kogai T, Sajid-Crockett S, Newmarch LS, Liu YY, Brent GA. Phosphoinositide-3-kinase inhibition induces sodium/iodide symporter expression in rat thyroid cells and human papillary thyroid cancer cells. *J Endocrinol.* 2008; 199: 243–252. doi: [10.1677/JOE-08-0333](#) PMID: [18762555](#)
48. Liu YY, Zhang X, Ringel MD, Jhiang SM. Modulation of sodium iodide symporter expression and function by LY294002, Akti-1/2 and Rapamycin in thyroid cells. *Endocr Relat Cancer.* 2012; 19: 291–304. doi: [10.1530/ERC-11-0288](#) PMID: [22355179](#)
49. Liu Z, Xing M. Induction of sodium/iodide symporter (NIS) expression and radioiodine uptake in non-thyroid cancer cells. *PLOS ONE.* 2012; 7: e31729. doi: [10.1371/journal.pone.0031729](#) PMID: [22359623](#)
50. Downward J. Mechanisms and consequences of activation of protein kinase B/Akt. *Curr Opin Cell Biol.* 1998; 10: 262–267. PMID: [9561851](#)